Green Chemistry

TUTORIAL REVIEW

View Article Online
View Journal | View Issue

Cite this: *Green Chem.*, 2018, **20**, 2412

Heterogeneous non-mercury catalysts for acetylene hydrochlorination: progress, challenges, and opportunities

Jiawei Zhong, [a,b,d] Yunpeng Xu*[a] and Zhongmin Liu *[a,c]

The replacement of mercuric chloride with non-mercury catalysts in acetylene hydrochlorination for the production of a vinyl chloride monomer (VCM), the precursor to polyvinyl chloride (PVC), would meet the requirements of green chemistry. The aim of this tutorial review is to discuss the design criteria for non-mercury catalysts, with the focus on the relationship between the catalytic activity/stability and the electronic properties, adsorption, and reducibility of the catalysts. The developments of Au-based catalysts, Ru-based catalysts and other monometallic catalysts are briefly covered in the first part, with emphasis on the active species, reaction mechanism, and alternative preparation methods of Au-based catalysts. An overview of the development of bimetallic/trimetallic catalysts is highlighted in the second part. Then the modification strategies (*e.g.* heteroatom modification of support, ionic liquid modification) and explorations of the support/preparation method are addressed. Finally, particular attention is paid to the applications of metal-free catalysts and other catalysts (*e.g.* heteroatom-doped carbon material, nitride and zeolite).

Received 8th March 2018,
Accepted 18th April 2018

DOI: 10.1039/c8gc00768c

rsc.li/greenchem

1. Introduction

Polyvinyl chloride (PVC), as the third most widely produced polymer after polyethylene and polypropylene, has a plethora of applications in the building and construction industry as well as in the packaging, electrical and apparel industries.[1–4] According to Ceresana, over 42 million tonnes of PVC were consumed globally in 2016, corresponding to over 16% of total plastics demand. It is anticipated that the global PVC demand will grow with an annual rate of 2.3% until 2024.[5] PVC is commonly produced through the polymerization of the vinyl chloride monomer (VCM). As shown in Fig. 1, there are two main industrial processes for the production of VCM, the acetylene method (also called the calcium carbide method) and the ethylene method. On one hand, VCM can be produced through direct acetylene hydrochlorination, with acetylene produced *via* calcium carbide CaC_2 from coal. On the other hand, VCM can be produced by the chlorination or oxychlorination of ethylene to 1,2-dichloroethane (EDC), and the thermal dehydrochlorination of EDC.[2,4,6] In the Western world, the production of VCM is based exclusively on ethylene-based processes, due to the well-developed olefins technology in the petrochemical industry, the loss of cost competitiveness of the acetylene-based technology as well as the concerns about the safety issues of handling acetylene on an industrial scale.[3] By contrast, the one-step acetylene hydrochlorination, as one of the most important coal-to-chemical applications, has

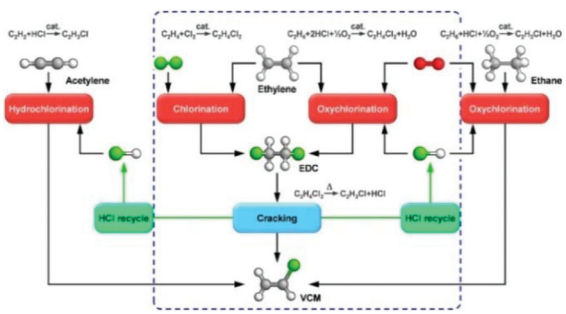

Fig. 1 Production of VCM from acetylene, ethylene, and ethane *via* hydrochlorination, chlorination, or oxychlorination. Reprinted with permission from ref. 6 Copyright 2017 American Chemical Society.[6]

[a]*National Engineering Laboratory for Methanol to Olefins, State Energy Low Carbon Catalysis and Engineering R&D Center, Dalian National Laboratory for Clean Energy, iChEM (Collaborative Innovation Center of Chemistry for Energy Materials), Dalian Institute of Chemical Physics, Chinese Academy of Sciences, Dalian 116023, PR China. E-mail: liuzm@dicp.ac.cn, xuyp@dicp.ac.cn; Fax: +86411 84691570; Tel: +86 411 84379335*

[b]*State Key Laboratory of Fine Chemicals, PSU-DUT Joint Center for Energy Research, School of Chemical Engineering, Dalian University of Technology, Dalian 116024, PR China*

[c]*State Key Laboratory of Catalysis, Dalian Institute of Chemical Physics, Chinese Academy of Sciences, Dalian 116023, PR China*

[d]*University of Chinese Academy of Sciences, Beijing 100049, PR China*

attained great interest in regions with plentiful and cost-effective coal supplies but a shortage of oil and gas (*e.g.* China).[3,7] The production capacity of PVC in China in 2017 has reached about 23 million tons, with approximately 80% PVC production coming from the acetylene route, occupying about 40% of the global production capacity of PVC.[8,9]

Currently, activated carbon (AC) supported mercuric(II) chloride catalyst with typically 10–15 wt% $HgCl_2$ is widely applied in the commercial acetylene hydrochlorination. However, the toxic and hazardous mercury chloride catalyst has many disadvantages, for example, the sublimation and loss of the active component due to the hot spots (>200 °C) in industrial fixed bed reactors ($C_2H_2 + HCl \rightarrow CH_2 = CH_2Cl$ $\Delta H = -124.8$ kJ mol^{-1}), the environment pollution associated with the catalyst manufacture, utilisation and disposal. In addition, according to the requirement of the Minamata Convention on Mercury passed by the United Nations Environment Programme (UNEP), the use of mercury per unit production should be reduced by 50% by 2020 against 2010, and the application of mercuric chloride catalyst in the PVC industry will be forbidden five years after the mercury-free catalysts based on the existing processes become technically and economically feasible.[10,11] Therefore, the dependence on mercury-containing catalysts has been the bottleneck that constraints the development of the acetylene-based PVC industry, and the replacement of the environmentally non-friendly mercuric chloride catalyst with a mercury-free catalyst can effectively solve the bottleneck in terms of green chemistry.[12–15] The developments of Au-based catalysts for acetylene hydrochlorination to VCM production have been reviewed by Hutchings *et al.*,[16–25] and the advances of mercury-free catalysts have also been outlined by Dai *et al.*[26,27] In addition, acetylene hydrochlorination has been discussed from the aspects of halogen chemistry[6] and acetylene-based chemicals.[28] However, considering the requirement of the Minamata accord, as well as the ever-increasing interest in acetylene hydrochlorination from both the academic and industrial fields, there is still a great necessity to summarize the green development of heterogeneous non-mercury catalysts for the manufacture of VCM. The aim of this tutorial review is to discuss the design criteria for non-mercury catalysts, with the focus on the relationship between the catalytic activity/stability and the electronic properties, adsorption and reducibility of the catalyst. The development of monometallic catalysts (*e.g.* Au-based and Ru-based catalysts), bimetallic and trimetallic catalysts, metal-free catalysts as well as the common modification strategies for acetylene hydrochlorination will be comprehensively reviewed.

2. Monometallic catalysts

2.1 Au-Based catalysts

Gold catalysis has played a vital role in a variety of applications such as low temperature CO oxidation, acetylene hydrochlorination, direct synthesis of hydrogen peroxide, propene epoxidation and selective oxidation.[29–41] For the acetylene hydrochlorination, by comparison with the environmentally non-friendly, highly toxic, easily volatile mercury(II) chloride catalyst, which also yields small amounts of 1,2-dichlorethane due to the sequential addition of hydrogen chloride to vinyl chloride, Au-based catalysts usually exhibit a quite high VCM selectivity >99.5% in acetylene hydrochlorination.[6,16,22] Moreover, it has been found that the catalytic activity generally decreases in the following order: gold > other precious metals > non-precious metals > non-metallic materials. Therefore, in this section, Au-based catalysts will be briefly addressed since the discovery, development and commercialization of Au-based catalysts for acetylene hydrochlorination have been com-

Jiawei Zhong

Jiawei Zhong completed the graduate course at University of Science and Technology of China (USTC) in 2013, joined Guangzhou Institute of Energy Conversion (GIEC) and received his M.S. from University of Chinese Academy of Sciences (UCAS) in 2015. He gave up the opportunity to join Eindhoven University of Technology (TU/e) with financial support from China Scholarship Council, and joined Dalian National Laboratory for Clean Energy (DNL), Dalian Institute of Chemical Physics (DICP), Chinese Academy of Sciences (CAS). He is pursuing his Ph.D. from Dalian University of Technology (DUT). His research interests include the methanol to olefin conversion, the catalytic conversion of biomass into chemicals and the non-mercury catalysts for acetylene hydrochlorination.

Yunpeng Xu

Yunpeng Xu was born in 1973 in Dalian (China). He received his Ph.D. degree in 2001 from Dalian Institute of Chemical Physics (DICP), Chinese Academy of Sciences, under the supervision of Prof. Liwu Lin. He was promoted to Full Professor of DICP in 2009. He is dedicated to the development of catalysts and new catalytic processes. His current research interests include synthesis of molecular sieves and development of non-mercury catalysts for acetylene hydrochlorination. He has authored more than 60 scientific publications and 80 patents.

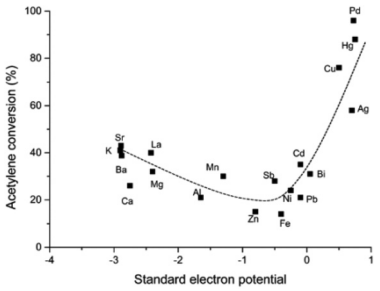

Fig. 2 Correlation of activity for acetylene hydrochlorination of carbon supported metal chloride with the standard electrode potential. Reproduced from ref. 45 with permission from The Royal Society of Chemistry.[17,45]

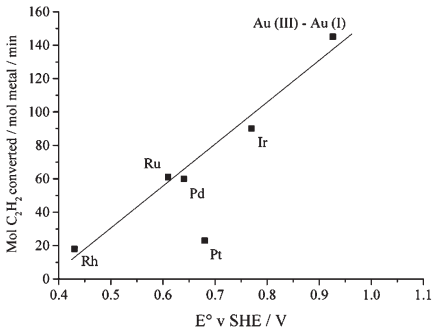

Fig. 3 Correlation between the activity for acetylene hydrochlorination and the standard electrode potential.[61] Potentials are obtained from the reduction potentials of $(RhCl_6)^{3-}$, $(RuCl_5)^{2-}$, $PdCl_2$, $(PtCl_6)^{2-}$, $(IrCl_6)^{3-}$ (all potentials for a 2 e^- reduction) and $(AuCl_4)^-$ to $(AuCl_2)^-$. Reproduced from ref. 61 with permission from The Royal Society of Chemistry.

prehensively reviewed by Hutchings[16–25] or other researchers.[42]

2.1.1 Active species. In the late 1980s, Hutchings *et al.* firstly correlated the catalytic activity of supported metal chloride catalysts with the standard electrode potential, instead of the electron affinity of the metallic cations previously reported by others,[43,44] predicted and verified that Au(III) cations with a higher electrode potential (1.42 V) than Hg(II) (0.7961 V) should provide enhanced catalytic activity in acetylene hydrochlorination (Fig. 2).[45–47]

Hutchings *et al.* demonstrated that Au/C deactivate at high temperatures (120–180 °C) due to the reduction of Au(III) or Au(I) to Au(0), as confirmed by ^{197}Au Mössbauer spectroscopy.[48,49] The deactivated Au/C can be reactivated online by cofeeding oxidising agents (Cl_2, NO, N_2O),[48] as well as offline by aqua regia treatment, as investigated in detail by X-ray photoelectron spectroscopy (XPS) and ^{197}Au Mössbauer spectroscopy.[50,51] Furthermore, the exposure of Au/C to C_2H_2 (a well-known reducing agent) results in the catalyst deactivation, whereas the exposure to HCl leads to enhanced activity, which might be due to the regeneration/activation role of HCl treatment that oxidizes Au(0) to some extent.[52] Therefore, Hutchings *et al.* proposed that Au(III) cations function as the active site in the Au/C catalyst. Meanwhile, some research groups postulated that Au(I)[53,54] and Au(0)[55–58] are the active species. Hutchings *et al.* further demonstrated Au(III) cations located at the Au/C interface should be the active species, since an excess of Au(III) cations exerts no contribution to the catalytic activity.[51,59,60] More recently, Hutchings *et al.* reported that the fresh catalyst prepared from aqua regia comprises atomically dispersed cationic Au species bound to the support rather than Au(0) nanoparticles, and the cationic Au (III) species *in situ* yields a Au(III)–Au(I) redox couple after reacting with acetylene and HCl, confirmed by high-angle annular dark-field-scanning transmission electron microscopy (HAADF-STEM), XPS and the sequential feeding test of a HCl/C_2H_2 mixture, HCl and C_2H_2.[17,61] And a correlation between the catalytic activity and the standard electrode potential based on Au^{3+}–Au^+ rather than the Au^{3+}–Au^0 redox couple was proposed (Fig. 3).

Considering the potential sample damage (*e.g.* photoreduction of Au(III) species during XPS analysis),[62] and the fact that the *ex situ* characterisation techniques cannot unambiguously provide the vital information on the active site, Hutchings *et al.* performed the first *in situ* X-ray absorption fine structure (XAFS) spectroscopy under operating conditions, and demonstrated that the highly active catalysts comprise highly dispersed single-site Au(I) species, and the catalytic activity is correlated strongly with the ratio of the Au L3-edge white-line intensity decided by the Au(I) : Au(III) ratio, and a redox mechanism between Au(I) and Au(III) was proposed and confirmed (Fig. 4).[17,63]

2.1.2 Reaction mechanism. The acetylene hydrochlorination is believed to proceed *via* the Eley-Rideal mechanism in which the gas phase HCl reacts with the adsorbed C_2H_2 on the catalyst surface.[64–67] DFT calculation indicates that C_2H_2 is a better ligand than HCl,[52,64] thus C_2H_2 is firstly adsorbed and

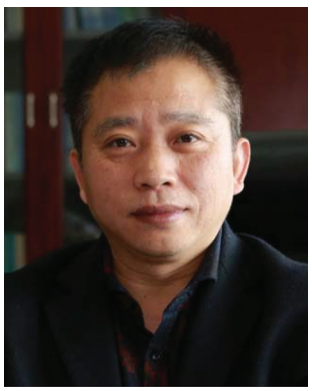

Zhongmin Liu

Professor Zhongmin Liu has been the Director of Dalian Institute of Chemical Physics, CAS since 2017. In 2006, as a leading scientist, Professor Liu successfully accomplished the industrial demonstration test of DMTO technology. Based on DMTO technology, the world's first commercial MTO unit was built by Shenhua group, which was a milestone for coal to chemicals. He published more than 300 papers, and applies more than 600 patents. He is the member of International Academic Committee of 13th, 14th and 17th International Zeolite Conference. He has received many awards such as the National Technological Invention Awards First Prize of China (2014), and the Science and Technology Innovation Award of the HLHL Foundation (2015). He was elected academician of the Chinese Academy of Engineering in 2015.

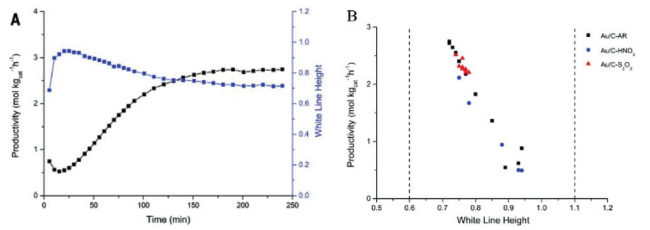

Fig. 4 VCM productivity and *in situ* characterization of the catalysts as a function of time-on-line. (a) Catalytic performance of the 1% Au/C-AR (black) and the change in normalized white-line intensity (blue). (b) Correlation between the variation in the Au L_3 white-line intensity and VCM production (Au/C-AR, Au/C-HNO_3 and Au/C-S_2O_3) (reproduced from ref. 63 with permission from the American Association for the Advancement of Science).

activated on the catalyst to form a C_2H_2-metal complex, then the gas phase HCl was added to the activated C_2H_2 to form C_2H_3Cl, which is considered the rate-determining step,[45,64,68–71] and the addition of HCl was shown to occur in the anti-stereochemistry configuration to acetylene and in accordance with the Markovnikov rule;[33,52] eventually, the C_2H_3Cl desorbs from the surface of the catalyst. The timely and sufficient supply of gas phase HCl is significant to maintain the catalytic activity, since the intermediate chlorovinyl is difficult to desorb from the $AuCl_3$ by converting to C_2H_3Cl due to the high desorption energy.[72] In addition, in the nucleophilic–electrophilic interaction between the electrophilic Au^{3+} center and the nucleophilic C_2H_2 *via* π-coordination,[52,73] if HCl could not interact with the activated C_2H_2 timely and sufficiently, the electron transfer from C_2H_2 results in the reduction of Au^{3+} to metallic Au^0 by losing Cl atoms,[72] and the activated C_2H_2 or reaction intermediate would easily polymerize to form coke deposition.[69]

2.1.3 Deactivation and regeneration. In general, the main reasons for the deactivation of Au-based catalysts include: (i) the reduction of active Au^{3+} or Au^+ species to Au^0 species, (ii) the occurrence of coke deposition and (iii) the aggregation of gold particles/clusters.[19,26]

Carbon-supported $AuCl_3$ catalysts suffer from deactivation at both high temperature and low temperature. The deactivation of Au/C at high temperatures (120–180 °C) is ascribed to the reduction of Au(III) or Au(I) to Au(0), while the deactivation at low temperatures (60–100 °C) is caused by the deposition of polymeric carbonaceous materials, probably resulting from the surface polymerization of vinyl chloride.[48,49] In addition, the deactivated Au/C can be reactivated off-line by aqua regia treatment,[50,51] as well as online by cofeeding oxidising agents (Cl_2, NO, N_2O),[48] both of which effectively reoxidize Au(0) to Au(I) and Au(III). And the coke residuals can be removed by an air oxidation process.[48] However, the aqua regia treatment introduces strong acid sites, which can result in the acetylene polymerization and the formation of carbon-containing nanotubes on the catalyst surface.[74] Recently, Yuan *et al.* reported that the iodohydrocarbon treatment under mild conditions not only reoxidizes the Au^0 species, but also redisperses large sintered Au particles to highly dispersed nanoparticles *via* the adsorption of iodic species on Au particles; iodides exhibit a better redispersion effect than alkyl chlorides and bromides,[75] and CHI_3 with low C–I bond dissociation energy effectively restores the activity of the Au/C catalyst in acetylene hydrochlorination.[76]

2.1.4 Preparation. The industrial application of aqua regia encounters a lot of disadvantages such as the corrosivity, hazard and potential environmental pollution. Moreover, the Au-based catalyst prepared from aqua regia exhibits an unsatisfactory stability owing to the reduction of the active species, the catalyst sintering as well as the side reaction associated with the acid sites on the catalyst.[16,17,49,74] In the past few years, a great amount of effort has been focused on the exploration of alternative gold precursors such as the Au complex, in order to prevent the use of aqua regia in the preparation and to enhance the stability of the active site under reaction conditions. The catalytic performances of Au-based catalysts from the Au-complex are summarized in Table 1.

In 2010, Jacobs has commissioned a pilot plant by a VCM manufacturer in western China, which replicated exactly a single tube reactor of the same dimensions as a full scale commercial VCM reactor (3 m × 50 mm diameter, with 2 kg catalyst charge).[77] Considering that the gold complexes with ligands containing soft donor atoms (*e.g.* thiosulfate, thiocyanate, thiourea, cyanides) display a greater stability in Au^+ and Au^{3+} than the counterpart with hard donor ligands (*e.g.* halides, nitrogen and oxygen atoms) that tend to disproportionate or be reduced to Au^0,[16,78] the team employed a series of sulphur-containing ligands (*e.g.* Au-thiosulfate, Au-thiocyanate, Au-thiourea) for the preparation of cationic gold complexes, and found a highly active and selective Au/C with 0.1% loading prepared by the immobilized $Na_3Au(S_2O_3)_2$ from aqueous solution on carbon extrudates (Fig. 5). The sulfur-containing ligands

Table 1 The catalytic performances of Au-based catalysts from the Au-complex

Catalyst	Electron trans.	Adsorp./desorp	Temp., °C	GHSV, h^{-1}	Conv., %	Time, h	Ref.
0.25%Au-SCN	√		180	1200	>95	3000	80
0.5%Au1-GSH3/AC		√	170	360	82	3	53
0.4%Au($CS(NH_2)_2)_2$/AC	√	√	170	870	>70	20	81
0.2%Au/Cu/TCCA			180	90	98	24	82
0.5%Au1Cu1SH10/AC	√		180	1200	56.3	8	56
0.49%[$AuCl_2$(phen)]Cl	√		180	280	>90	40	83
0.5%AuPPh_3Cl/AC	√	√	170	360	85	200	84

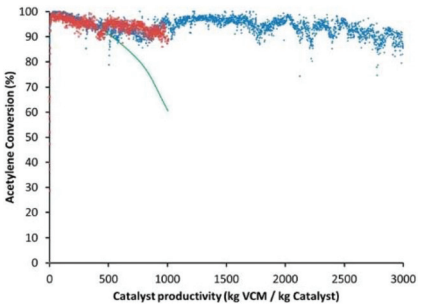

Fig. 5 Comparison of catalyst performance in a primary reactor for a 10% $HgCl_2$/C catalyst (green), pilot plant operation for 0.1% Au/C to a yield of 3000 kg VCM kg^{-1} catalyst (blue), a full scale commercial reactor for 0.1% Au/C to a yield of 1000 kg VCM kg^{-1} catalyst (red). Catalyst = 0.1% Au/C prepared by supporting $Na_3Au(S_2O_3)_2$ on carbon extrudates. Typical yield for 10% $HgCl_2$/C catalyst = *ca.* 1000 kg VCM kg^{-1} catalyst. Reprinted with permission from ref. 16 Copyright © 2015 American Chemical Society.[16]

stabilize the cationic gold, which prevent the catalyst from fast deactivation, and the aqua regia is not required during the catalyst preparation.[17,78] Throughout the operation of the pilot plant, the catalyst conversion was >85%, and the catalyst selectivity was >99%. In 2012, a full-scale shell and tube reactor with 790 tubes was constructed. The reactor was loaded with 1.6 t Au/C catalyst and was run for more than 4500 h. The conversion was >90%, and the selectivity was >99%.[16,29] The catalyst is currently marketed as part of the Johnson Matthey's PRICAT catalyst and is applied in the only mercury-free process currently offered for license (DAVY VCM process).[79]

In 2014, Wei and co-workers prepared 0.25 wt% Au-based catalyst by complexing Au cations with thiocyanate (–SCN).[80] –SCN decreases the electrode potential of Au(III) cations from 0.926 V to 0.662 V, and prevents the Au catalyst from quick deactivation by the reduction by C_2H_2. The 3000 h industrial testing on a 4 t per annum scale verified the catalyst's long-term stability, promising reactivity (>95%) and selectivity (>99%) (Fig. 6).

Other sulphur-containing ligands have also been explored. For example, Zhang *et al.* found that the glutathione (GSH) addition leads to the reduction of Au^{3+} to Au^{+}, and Au-GSH/AC enhances the chemical adsorption of HCl, and proposed that the Au^{+} species effectively enhances the catalytic activity.[53] Additionally, Zhu *et al.* prepared 0.4 wt% $AuCl_3$-thiourea/AC catalyst and proposed that the electron transfer from thiourea to the Au center increases the quantity of Au^{+} and Au^{3+} species, which leads to the enhanced adsorption of HCl.[81] Luo *et al.* found that the addition of trichloroisocyanuric acid (TCCA) enhances the long-term stability of 0.2 wt% Au/Cu/TCCA catalyst, and 6800-h pilot-trial evaluation was performed and the promising capability for future practical applications was verified (Fig. 7).[82] Through DFT calculation, they proposed that the weakened interaction between Au and acetylene over Au/Cu/TCCA results in a negative adsorption energy

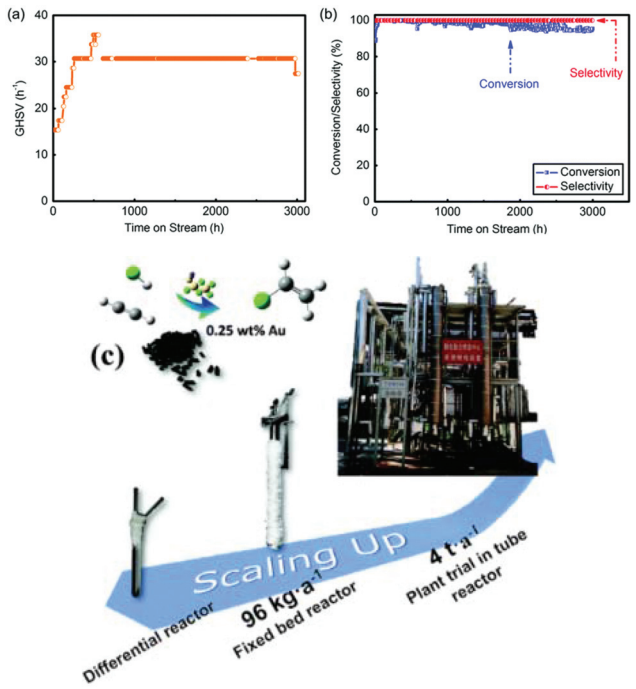

Fig. 6 (a) GHSV during the evaluation of the pilot-trial analysis; (b) conversion and selectivity in 3000 h evaluation. (c)The fixed bed reactors in different scales: the U-shaped silica tube with 6 mm inner diameter loaded with 0.15 g catalyst, the fixed bed reactor with 30 mm inner diameter loaded with 60 g catalyst and the single tube fixed bed reactor with 80 mm inner diameter loaded with 2.5 kg catalyst. Reproduced from ref. 80 with permission from The Royal Society of Chemistry.[80]

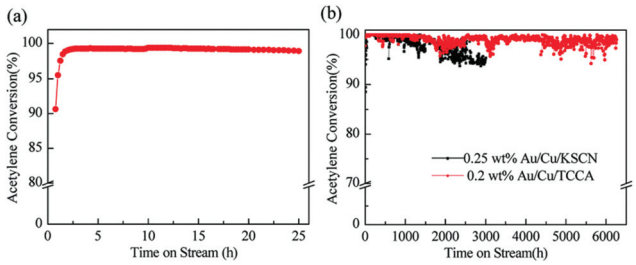

Fig. 7 (a) 25 h laboratory evaluation of 0.2 wt% Au–Cu catalysts with Au : Cu : TCCA = 1 : 5 : 20 (mole ratio), reaction conditions: T = 180 °C, GHSV = 90 h^{-1}. (b) Comparison of 6800 h pilot-trial evaluation between Au/Cu/TCCA and Au/Cu/KSCN systems, reaction conditions: T = 180 °C, GHSV = 30 h^{-1}. Reproduced from ref. 82 with permission from The Royal Society of Chemistry.

(−570.35 kJ mol^{-1}), which inhibits the reduction of high valence Au by acetylene and the coking effect caused by acetylene polymerization.

Meanwhile, some researchers switch the attention to nitrogen-containing ligands. For instance, Dai and co-workers reported that the Au(III)/Schiff-based catalyst $[AuCl_2(phen)]Cl$ exhibits enhanced catalytic activity and stability, which is ascribed to the inhibited reduction of Au^{3+} to metallic Au^{0} by the electron transfer from the 1,10-phenanthroline ligand to

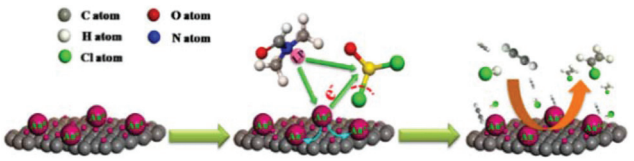

Fig. 8 Proposed oxidative dissolution mechanism for Au in OAR. © 2017 Elsevier Inc. All rights reserved.[85]

the Au^{3+} center.[83] Similarly, Zhang *et al.* prepared a triphenylphosphine (TPP)-ligated Au-based catalyst ($AuPPh_3Cl$/AC); the TPP increases the electron density of Au^{3+} and Au^{+} through electron transfer, the strong coordination effect enhances the stability of Au^{3+} and Au^{+} species and inhibits the reduction of Au^{3+} or Au^{+} species to Au^{0} species.[84] The TPP ligand enhances the HCl adsorption and weakens the C_2H_2 and VCM adsorption, which results in improved catalytic activity and long-term stability.

Likewise, considering the corrosivity, hazard and potential environmental issues of aqua regia,[51] Li *et al.* employed the less toxic, relatively safe, and recyclable organic aqua regia (OAR),[85] the simple mixtures of thionyl chloride ($SOCl_2$) and *N*,*N*-dimethylformamide (DMF).[86] OAR can not only activate and increase the catalytic activity of Au/AC prepared from aqueous $HAuCl_4$, but also reactivate the used catalyst. The residual sulfur atoms may form Au–S complexes while the residual nitrogen atoms may increase the electron density of the Au center through electron transfer, which increases the reduction temperature of the Au^{3+} species, and stabilizes the cationic Au^{3+} species (Fig. 8). Moreover, the electron-rich catalyst treated with OAR enhances the adsorption of HCl and weakens C_2H_2 chemisorption strength, which also prevents the reduction of the active Au^{3+} species caused by C_2H_2.[87]

2.2 Other monometallic catalysts

Considering the relatively high price of Au, ever-increasing interest has been shown in the exploration of other noble metal based or non-precious metal based catalysts for acetylene hydrochlorination. In 2012, Kang *et al.* employed density functional theory (DFT) to calculate the activation barrier of the catalysts MCl_x (M = Hg, Au, Ru; x = 2, 3) for acetylene hydrochlorination,[68] and found that the activation barriers were 16.3, 11.9, and 9.1 kcal mol^{-1} for $HgCl_2$, $AuCl_3$, and $RuCl_3$, respectively, indicating that Ru-based catalysts may be a good candidate for the acetylene hydrochlorination. Considering the merits of Ru such as low price, high activity, and environmental benignity, many groups have been engaged in the study of Ru-based monometallic catalysts. For instance, Li *et al.* found that the content of RuO_2 plays a positive role in the activity in the acetylene hydrochlorination over a spherical activated carbon (SAC) supported Ru-based catalyst (Ru/SAC), and proposed that RuO_2 is the major active ingredient in the oxidative treatment.[88] Similar conclusions that RuO_2 acts as the active component have also been drawn by other researchers.[69,89–91] Zhang and co-workers reported that Ru-based catalysts with nanoparticles confined in CNT channels (Ru-in-CNT) exhibit better catalytic activity, by comparison with that with particles deposited outside of CNTs (Ru-out-CNT).[92] They proposed the electron transfer from the ruthenium species in the channel of CNTs to the electron-deficient interior surface of CNTs, which leads to the dominant formation of RuO_2 in Ru-in-CNTs.

In addition, attention has been paid to Pt-based,[93–96] Rh-based,[97] Ag-based,[47] and Pd-based[70,98] (*e.g.* Pd/NH_4F-HY,[99] Pd/NH_4F-Urea-HY,[100] Pd/PANI-HY,[101] Pd NPs/tetrabutylphosphonium stearate[102]) catalysts, in particular, the cost-effective non-precious metal-based catalysts including Cu-based (Cu-NCNT,[103] CuP/SAC,[104] $CuCl_2$-[Bmim]Cl[105]), Co-based (Co–N-AC[106]) and Bi-based (BiP/AC[107]) catalysts, with some catalytic systems deeply discussed in the corresponding section 4.1 (heteroatom modification of support) and section 4.2 (ionic liquid modification).

3. Bimetallic or trimetallic catalysts

Hutchings *et al.* once reported that the noble metal addition (Pd, Pt, Ir, Rh and Ru) exhibited little positive effect on the acetylene hydrochlorination, and the lower activity of bimetallic Au-based catalysts is attributed to the lower standard electrode potential.[108] However, in recent decades, a variety of bimetallic or trimetallic catalysts by the introduction of a second metal chloride or metal oxide have been developed so as to reduce the gold content and to improve the catalytic activity/stability. The addition of other metal chlorides or metal oxides usually increases the catalytic activity/stability through the following directions:

(1) stabilize the catalytically active species (*e.g.* Au^{3+} or Au^{+} species for Au-based catalysts, RuO_2 for Ru-based catalysts[91,109]), and inhibit the reduction of the active component (*e.g.* Au^{3+} or Au^{+} species to Au^{0}), confirmed by the increased relative amount of active species (XPS,[91,109–113] H_2-TPR[109,114,115]), the increased reduction temperature of active species (H_2-TPR),[91,110,111,114–118] the increased reduction activation energy of Au^{3+} to Au^{0},[111] or the increased content of C_2H_2 desorption that has access to the active site (C_2H_2-TPD).[114,115,119]

(2) increase the electron density of active species through electron transfer from the additive to the active species (negative binding energy shifts confirmed by XPS),[112,120–123] which strengthens the chemisorption of HCl over the electron-rich catalyst (HCl-TPD),[54,62,114,117] and the adsorbed HCl can help the metal species maintain the corresponding oxidative state, and inhibit the reduction of active species by C_2H_2.[52,72] However, it should be noted that the interaction between the promoter and active species might also result in the lower reduction temperature of active species (H_2-TPR).[54,110,113,117,120,123] Likewise, enhancing the desorption of the VCM (C_2H_3Cl-TPD)[109] can also increase the long-term stability, since the adsorbed VCM can lead to the formation of carbonaceous materials *via* polymerization.[49]

Table 2 Catalytic performance of bimetallic or trimetallic catalysts

	Catalyst	Electron transfer	Adsorp./ desorp.	Anti coke	TOF	V(HCl /C_2H_2)	Temp. °C	GHSV h^{-1}	C_2H_2 conv., %	Time h	Stability h	Ref.
Au-based	1Au(1%)–5Y/AC		√	√		1.2	180	800	65.9	110	2300 (30 h^{-1})	125
	Au(0.1%)–Cu-IL/AC	√	√		168.5 h^{-1}	1.2	180	50	98.5	500		62
	Au(0.2%)/Cu/TCCA	√		√		1.1	180	90	98	24		82
	Au(1%)1Sr(II)1/AC	√	√	√	2.8 s^{-1}	1.15	180	762	87.7	20		112
	Au(0.25%)Cu(4%)/C		√	√		1.1	150	720	97.4	150		111
	Au1(1%)Sn1/AC	√	√	√	657 min^{-1}	1.1	170	720	95	48		120
	$AuCl_3$–$CuCl_2$/γ-Al_2O_3					1.1	150	120	≈90	6		126
	1Au(1%)–4Cs^I/AC		√		0.27 s^{-1}	1.2	180	50	99.8	500		115
	1Au(1%)–1Ba(II)/AC	√	√	√		1.15	200	360	97.2	48		114
	1Au(0.3%)–3Bi/AC	√			184 h^{-1}	1.1	180	600	85	5		54
	Au(0.1%)–5Bi/γ-Al_2O_3	√				1.05	150	120	96	10		118
	1Au(1.5%)–3Ni/CSs	√		√		1	170	900	95.4	46		116
	1Au(1%)–1La(III)/SAC			√		1.15	150	360	87.6	36		110
	1Au(1%)–1Co(II)/SAC			√		1.15	150	360	88.8	36		
	1Au(1%)–3Co(III) /SAC			√		1.15	150	360	92	48		
	1Au(1%)–3La/SAC			√		1.15	150	360	90	48		127
	1Au(0.5%)–5Cu/C					1.15	160	50	99.5	200		64
	1Au(1%)–5CeO_2/AC	√	√	√		1.15	180	852	98.4	20		123
	1$AuCl_3$(1%)–10TiO_2/AC	√	√			1.15	180	870	81	10		122
	Au(0.2%)–Cu–K/AC					1.05	165	40	89	1600		128
	Au(1%)In^{III}(1%)Cs^I(4%)/AC	√	√	√		1.2	180	1480	89.1	50	6520 (50 h^{-1})	117
	1Au(0.25%)1Cu4Cs/AC	√	√	√		1.2	180	50	98.8	600	6540 (30 h^{-1})	119
	1Au(1%)3Co(III)1Cu(II)/SAC	√	√	√		1.15	150	360	99.7	48	6513 (30 h^{-1})	121
	Au(1%)–Cu(0.4%)-IL/AC	√	√		168.5 h^{-1}	1.2	180	740	76.7	12	500 (50 h^{-1})	62
Other	Ru(0.1%)1Co(III)3Cu(II)1/SAC			√		1.1	170	180	99	48	500 (90 h^{-1})	91
metal	1Ru(1%)–1K/SAC		√	√	2.45 min^{-1}	1.2	170	180	86.5	48		109
based	1Ru(1%)–3Co/SAC			√		1.1	170	180	95	48		129
	Cu(4.24%)–Ru(400 ppm)/CNTs				1.81 min^{-1}	1.2	180	30	≈85	65		113
	Pd–K(7%)/NFY	√		√		1.25	160	110	99	50		130
	Bi/Cu/H_3PO_4/Silica gel					1.05	200	360	≈80	200		131

(3) facilitate the dispersion of metal species[19,26] (confirmed by CO-TPD[91,109] and TEM[112,114,120]), and high dispersion of metallic species might provide more active sites.

(4) obstruct the reduction of the active component, and retard the agglomeration of nanoparticles to some degree, instead of completely inhibiting the catalyst sintering (particle size calculated by the Scherrer equation in XRD, TEM,[117] and STEM[62,91]).

(5) inhibit the coke deposition (verified by TGA and TPO[119]).

The influence of the additive on the electronic, adsorption, and redox properties of bimetallic or trimetallic catalysts is summarized in Table 2. And some representative studies are discussed in detail in the following. Zhang *et al.* reported that Co(III), Co(II) and La(III) additives stabilize the catalytically active Au^+ species and inhibit the reduction of Au^{3+} into Au^0, with the best catalytic performance achieved by Co(III) additives, which might be attributed to the higher standard electrode electric potential of Co(III), and the Au–Co(III) based catalyst effectively inhibits the occurrence of coke deposition.[110] Based on the fact that Au facilitates the reducibility of Ni(II) at relatively low temperatures,[124] Li *et al.* prepared a Au–Ni bimetallic catalyst, and proposed that the electron transfer from Au to Ni inhibits the reduction of Au^{3+} and Au^+ to Au^0, and oxidizes the reduced Au^0 to Au^+, which leads to enhanced catalytic activity, inhibited coke deposition and longer stability.[116] Wei *et al.* found that the Bi additive stabilizes the formation of AuCl by electron transfer from Bi^{3+} to Au^{3+}, and inhibits the reduction to metallic Au (confirmed by XPS, XANES and EXAFS spectra), which results in a high hydrochlorination TOF of 184 min^{-1} (Fig. 9).[54] However, it should be mentioned that $BiCl_3$ additives are highly volatile due to the low boiling points (350 °C).

Due to the low cost and good thermo-stability, Cu was often selected as the additive. Li *et al.* found that the supported-ionic-liquid-phase (SILP)-stabilized bimetallic catalyst (Au–Cu-IL/AC) exhibits excellent catalytic performance and long-term stability.[62] It is proposed that the addition of $CuCl_2$ not only

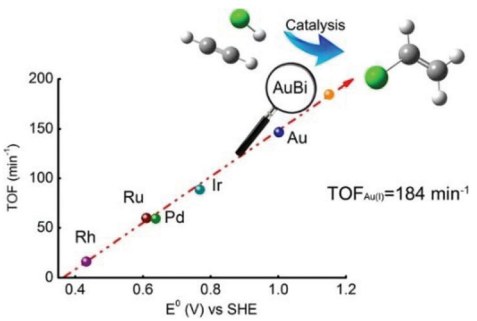

Fig. 9 Correlation between TOF values *versus* the standard electrode potential of AuBi and other metals. Reprinted with permission from ref. 54. Copyright 2014 American Chemical Society.[54]

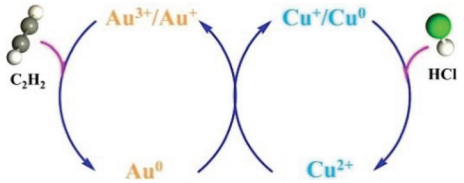

Fig. 10 Schematic representation of the proposed oxidative mechanism for Au^0 by Cu^{2+} over the Au–Cu-IL/AC. Reprinted with permission from ref. 62. © 2017 Elsevier B.V. All rights reserved.[62]

inhibits the reduction of Au^{3+} species, but also *in situ* re-oxidizes the reduced Au^0 species to cationic Au species. A coupled redox cycle involving the Cu^{2+} species was proposed, the reduced Au^0 species by C_2H_2 is re-oxidized *in situ* to the cationic Au species by Cu^{2+}, and then the formed Cu^0 is re-oxidized to Cu^+ by HCl, with the unstable CuCl transforming into metallic Cu^0 and $CuCl_2$ to complete the catalytic cycle (Fig. 10).

Likewise, trimetallic catalysts have also attracted great interest due to the synergistic effect between the additives and the active metal species. For example, Zhang and co-workers reported that the ternary Au–Co(III)–Cu(II) catalyst exhibits excellent catalytic performance and long-term stability due to the synergistic effects of Co(III) and Cu(II).[121] The Co(III) species with a higher standard electrode potential than Au^{3+} shows a stronger ability to adsorb HCl, thus stabilizing the active Au^+ species and inhibiting the reduction of Au^{n+} (n = 1 or 3) to Au^0. The Cu(II) species stabilize the high oxidation state of the Au^{3+} species by electron transfer and act as a co-catalyst. Moreover, Zhang and co-workers reported that satisfactory catalytic performance and long-term stability can be achieved over the Ru–Co(III)–Cu(II)/SAC catalyst.[91] The Co(III) additives interact strongly with Ru species and facilitate the formation of high valent ruthenium oxides. And the Cu(II) species inhibit the reduction of $RuCl_3$ precursors, and make Co^{2+} or Co^0 transform to high valent species of Co(III), which is beneficial for the formation of ruthenium oxides. Similarly, Li *et al.* reported that the synergistic effects among $AuCl_3$, $InCl_3$ and CsCl significantly enhance the activity and the stability of Au-based catalysts.[117] In particular, the $InCl_3$ additive, with less electronegativity than Au, increases the electron density of Au^{3+} species *via* the electron transfer from the In atom to the Au^{3+} center, and enhances the adsorption of HCl over the electron-rich catalyst.

In addition, some researchers investigated the catalytic performance of bimetallic or trimetallic catalysts in pilot-scale trials. For instance, Wei *et al.* conducted a 20-ton-per-year pilot-scale trial over 700 h in fluidized-bed reactors with high heat transfer efficiency and reported that the silica gel-supported Bi–Cu catalyst stabilized by H_3PO_4 exhibited around 80% C_2H_2 conversion in former 200 h.[131] Similarly, Zhao *et al.* conducted a long-run test of 1600 h over Au–Cu–K/AC in a fixed bed reactor by a single-tube pilot unit.[128] The synergy effect between the additive and gold facilitates the dispersion of the active species and inhibits coke formation, which leads to higher long-term stability.

However, it should be noted that the addition of other metallic promoters (*e.g.* K, Cs, *etc.*) will increase the recovery cost of the Au-based catalyst, since the recovery of Au can be easily achieved by dissolving in aqua regia.[26]

4. Modification strategies

4.1 Heteroatom modification of support

Due to the excellent electron conductivity and high specific surface area, carbon material has been widely adopted as the support for metal-based catalysts for the acetylene hydrochlorination. The dopants of non-metal elements (*e.g.* nitrogen, boron and phosphorus) in the carbon material effectively modify the surface chemistry and tune the electron affinity. Therefore, heteroatom modification including surface grafting or bulk doping is often adopted to enhance the stability of the active species. The catalytic performance of catalyst systems with heteroatom modification of the support (4.1), ionic liquid modification (4.2), or novel support (4.3) are summarized in Table 3. The heteroatom modification usually improves the stability of the active species through the following ways:

(1) It functions as the anchoring sites for the active component, stabilizes the catalytically active component (*e.g.* Au^{3+}/Au^+ species, RuO_2,[89,90] Cu^{2+}/Cu^+ species,[103,104] Pd^{2+} species[100,101]), and prevents the reduction of the active component, confirmed by the increased relative amount of active species (XAES,[104] XPS,[87,100,132] H_2-TPR[89,133,134]), the increased reduction temperature of the active species (H_2-TPR),[87,90,104,107,135,136] the increased reduction activation energy,[90] or the increased amount of adsorbed C_2H_2 that correlated with the amount of active component (C_2H_2-TPD).[133,136]

(2) It enhances the chemisorption of HCl (HCl-TPD),[106,133,135,136] due to the increased electron density of the active component *via* electron transfer from the heteroatom (negative binding energy shifts confirmed by XPS),[90,100,101,133] or decreases the adsorption of vinyl chloride (C_2H_3Cl-TPD).[89,90]

(3) It promotes the dispersion of the active component (CO-TPD,[90,134] N_2O chemisorption[104]), and retards the aggregation of active species (particle size calculated from the Scherrer equation from XRD, TEM,[107] STEM[135]).

(4) It retards the coke deposition (TGA).

For the first time, Dai *et al.* adopted nitrogen-doped CNTs prepared from the pyrolysis of polypyrrole (PPy) as a support for the Au-based catalyst ($AuCl_3$/PPy-MWCNTs), and attributed the enhanced catalytic activity to the electron transfer from the N atom of PPy to the Au^{3+} center and the increased adsorption of hydrogen chloride.[87] Afterwards, Li *et al.* deeply investigated the surface chemistry of the carbon support by liquid phase oxidation processes using concentrated HNO_3 solution and subsequent thermal treatments under different atmospheres (H_2/N_2) and temperatures. There is a strong correlation between surface oxygenated groups (SOGs) and catalytic performance, and the catalytic activity and stability of Au/AC can be improved by increasing the amounts of SOGs, especially phenol, ether, and carbonyl (Fig. 11).[137] The P doping comprising phosphate groups, $(PO_4)^{3-}$ and $(PO_3)^+$ from triphenylphosphine has also been adopted over Au/P-SAC.[132]

Table 3 Catalytic performance of catalyst systems with heteroatom modification of the support, ionic liquid modification, or novel support

	Catalysts	Temp., °C	GSHV, h^{-1}	Conv., %	Time, h	Ref.
4.1.1	$AuCl_3$/4PPy-CNT	180	100	>80	100	87
	Au/20%P-SAC	170	360	99.9	23	132
	Ru(1%)–O/AC–O	180	180	99.6	24	134
	Ru/AC-NHN	180	360	91.8	48	89
	Pd(0.9%)/2NH_4F-urea-HY	160	110	99	8	100
	Pd(0.9%)/PANI(40%)-HY	160	110	95	300	101
	2.5Cu(15%)P/SAC	140	30	97.2	82	104
	$BiP_{0.5}$/AC	160	120	67.5	9	107
	Bi/Cu/H_3PO_4	180	50	80	200	131
4.1.2	Au/NAC	180	100	99.9	300	133
	1Au4Cs/NAC	180	1480	98.6	50	135
	Ru/SAC-N700	170	180	99.8	30	90
	Co–N-AC	180	36	≈50	9	106
	Cu(5%)-NCNT	180	180	43.8	280	103
	Au(0.25%)/B(20%)AC	150	770	81.4	12	136
4.2	Pd NPs/[P4444][C17COO]	180	13.6	93	55	102
	0.1%Au–Cu-10%[Prmim]/AC	180	50	98.5	500	62
	0.2%Ru@15%TBPB/AC	170	90	99.3	400	69
	Ru10%[BMIM]BF_4/AC	170	180	98.9	24	143
	Au-5%[Prmim]/AC	180	30	95.7	300	142
4.3	Au/MCN	180	220	≈75	7	58
	0.5%$AuCl_3$/MC	180	720	84.7	8	146
	Au/AC-SiC	165	60	90	200	147
	1Au(1%)/5SiO_2/AC	180	530	≈70	16	148

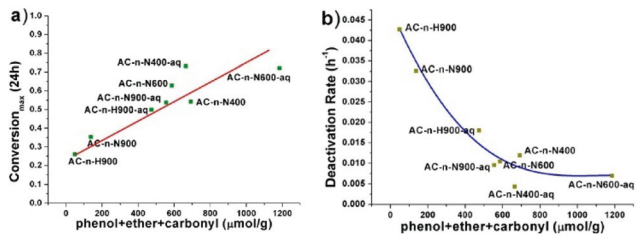

Fig. 11 Correlation between the amount of phenol, ether, and carbonyl and catalytic performance of catalyst: (a) the highest acetylene conversion in 24 h and (b) deactivation rate. Reprinted with permission from ref. 137. Copyright 2014 American Chemical Society.[137]

Furthermore, much attention has been paid to the influence of surface heteroatom modification for other monometallic or bimetallic catalysts. For example, the influence of oxygenated functional groups generated by HNO_3 treatment,[134] and nitrogen functional groups (–NO_2, –NH_2 and –N–H–N prepared from nitration, amination and pyridine)[89] on the activity/stability of Ru/AC has been studied. Likewise, nitrogen [polyaniline (PANI) as the precursor[101]], fluorine (NH_4F as the precursor),[99,130] or nitrogen and fluorine dually doped (NH_4F-urea modification)[100] zeolite HY have been investigated in Pd-based catalysis. As for non-noble metal catalysts, phosphoric acid modification has been applied for CuP/SAC,[104] $BiP_{0.5}$/AC,[107] and Bi/Cu/H_3PO_4/silica gel.[131]

By contrast, the heteroatom modification with bulk doping is also adopted to improve the stability of the active species. For instance, Li *et al.* reported that the bulk nitrogen doping of AC through thermal pretreatment with urea removes the carboxylic groups on the AC surface, which prevents the surface decarboxylation and the subsequent reduction of Au^{3+} to Au^0 over Au/NAC.[133,138] The coexistence of nitrogen species and phenolic groups functions as the anchoring site for the gold cations and stabilizes the Au^{3+} species. Meanwhile, the increased electron density of Au^{3+} species *via* electron transfer from nitrogen atoms to the Au^{3+} center enhances the adsorption of HCl and inhibits the reduction of Au^{3+} to Au^0. The effect of bulk nitrogen doping *via* the pyrolysis of the different precursors (*e.g.* urea for AuCs/NAC,[135] melamine for Ru/SAC-N,[90] 1,10-phenanthroline for Co–N-AC,[106]) or other methods [nitrogen doping in carbon sheets *via* chemical vapor deposition (CVD) for Cu-NCNT[103]] on the catalytic performance has also been widely investigated. In addition, Hu *et al.* reported that the boron bulk doping from the calcination of boric acid stabilizes the catalytically active Au^{3+} species over Au/BAC, inhibits the reduction of Au^{3+} to Au^0, and increases the adsorption of HCl, which results in the improved catalytic performance.[136] Meanwhile, the boron species effectively inhibits carbon deposition and catalyst sintering.

4.2 Ionic liquid modification

Currently, most of the catalytic hydrochlorination of acetylene is carried out in the gas-phase reaction.[1] While regional hotspots and carbon deposition easily occur in the gas-phase reactions, the liquid phase reaction is able to provide mild temperature control and heat removal. In recent years, much attention has been given to ionic liquids (ILs) due to merits such as the large solubility of metal-based catalysts, a wide liquid range, nearly negligible vapor pressures and thermal stability.[139–141] For instance, Cao *et al.* conducted the reaction with ILs (*e.g.* [Bmim]Cl, [Bmim]HSO_4, [Bmim]PF_6, [Emim]PF_6, [EPy]Br and [BPy]BF_4) as reaction media, and deeply investi-

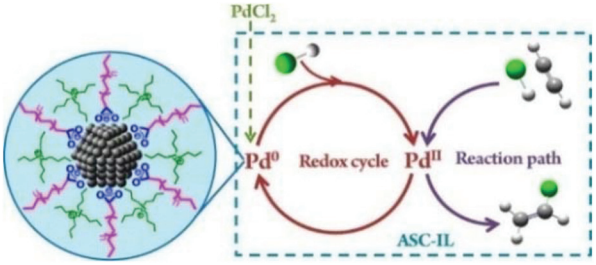

Fig. 12 Redox cycle between Pd^0 and Pd^{II} involved in acetylene hydrochlorination with an amplified microgram of a Pd NP. Reprinted with permission from Ref. 102. Copyright 2015 American Chemical Society.[102]

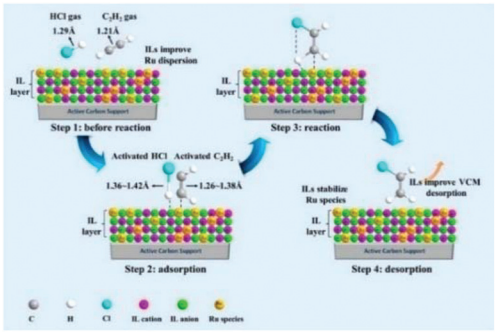

Fig. 13 Mechanism of acetylene hydrochlorination over Ru@IL/AC. Reprinted with permission from Ref. 69. Copyright 2017 American Chemical Society.[69]

gated the $CuCl_2$-[Bmim]Cl system.[105] Xing *et al.* designed Pd/Au/Pt nanoparticles (NPs)/anionic surfactant carboxylate IL (ASC-ILs) systems for the gas–liquid acetylene hydrochlorination, and satisfactory results were achieved over the Pd NPs/tetrabutylphosphonium stearate ([P4444][C17COO]) system.[102] A redox cycle between Pd^0 and Pd^{II} was proposed. Pd^0 is oxidized to Pd^{II} by reactant HCl to generate the catalytically active Pd^{II} component. With Pd^{II} catalysing the reaction of C_2H_2 and HCl, partial Pd^{II} is reduced to Pd^0 by C_2H_2. Meanwhile, the self-assembly property of long-chain ASC-ILs facilitates the *in situ* formation of Pd NPs from the reduced Pd^0 clusters and prevents the aggregation of NPs (Fig. 12). In addition, due to the strong hydrogen-bond basicity and good lipophilicity (weak polarizability), ASC-ILs effectively absorb and activate HCl, which enhance the catalytic activity.

More recently, the supported ionic liquid phase (SILP) technique has been adopted in acetylene hydrochlorination. ILs can effectively stabilize the catalytic species and prevent the active species from agglomeration. In addition, ILs can form a thin film on the catalyst surfaces that provides a homogeneous reaction medium for the highly dispersed metal complex, and enhance the adsorption of the reaction substrates to facilitate their access to the active sites.[62,142] Therefore, catalytic systems containing ILs such as Au(III)-IL/AC with the 1-propyl-3-methylimidazolium chloride ([Prmim][Cl]),[142] Ru-IL/AC with 1-butyl-3-methylimidazolium tetrafluoroborate ([BMIM]BF_4),[143] Au–Cu-IL/AC from [Prmim]Cl with strong hydrogen-bond basicity[62] have been explored. Additionally, Li *et al.* deeply investigated the reaction mechanism of the reaction over Ru@TPPB/AC.[69] The thin layer of TPPB on the surface of AC improves the dispersion of Ru species, stabilizes the active Ru species, and inhibits the reduction of the active Ru species. C_2H_2 is prior to be adsorbed and activated on the Ru species, while HCl gets electrons from ILs and activated by ILs. TPPB exhibits higher adsorption amount of HCl than that of C_2H_2, and the timely addition of HCl interacts with the activated C_2H_2, thus inhibiting the coke deposition caused by the polymerization of the activated C_2H_2 and reaction intermediate (*e.g.* $C_2H_3^{\bullet}$ or $C_2H_2Cl^{\bullet}$). Finally, the VCM is removed quickly from the interface of IL due to the weak adsorption ability of the IL for VCM, which also retards the coke deposition (Fig. 13).

4.3 Support/preparation method exploration

The dispersion of metal species plays a vital role in the catalytic activity and catalyst lifetime. Therefore, in addition to the conventional incipient wetness impregnation method, a range of other preparation methods (*e.g.* mixed solvents and vacuum-drying process,[55] ultrasonic-assisted impregnation[99–101,111,130,144] or the microwave-assisted method[144,145]) have been developed in recent years.

In addition, the coconut shell activated carbon (AC) with low mechanical strength is easily crushed under reaction conditions, resulting in the loss of active component and catalyst deactivation. Therefore, efforts are ongoing to replace AC with other supports, for example, pitch-based spherical activated carbon (SAC),[88,90,91,104,110,127] mesoporous carbon with interconnected mesoporous networks that facilitate the reactant molecular diffusion and reaction product transport,[146] mesoporous carbon nitride (MCN) with high thermodynamic stability,[58] silicon carbide (SiC) foam with high thermal conductivity, high mechanical strength and good chemical inertness,[147] mesoporous γ-Al_2O_3,[118,126] and silica modified activated carbon (SiO_2/AC).[148] Until now, there have not been sufficient reports considering the acidity/basicity of the support; silica with surface acidity was claimed to lead to polymerization products,[43,45] and mesoporous γ-Al_2O_3 with strong basic sites and further KOH modification was reported to enhance the catalytic activity.[126]

5. Metal-free catalysts and other catalysts

By comparison with metal-containing catalysts that suffer from sintering during the reaction, metal-free catalysts are not only cost-effective but also exhibit improved stability. In particular, heteroatom doped materials (*e.g.* heteroatom doped carbon, nitride) have gained substantial attention due to the unique chemical and electronic properties. In general, the electrophilic addition of HCl to acetylene is significantly influenced by the electron affinity of the active site.[149,150] The incorporation

of heteroatoms (*e.g.*, N, B, S) into the sp^2 hybridized network usually improves the catalytic performance through the following ways:

(1) It increases the electron density of the catalyst, which strengthens the chemisorption of HCl over the electron-rich catalyst (HCl-TPD),[151–157] enhances the adsorption ability of C_2H_2 that has access to the active site (C_2H_2-TPD),[67,152,154–160] or decreases the adsorption of vinyl chloride (C_2H_3Cl-TPD).[155,157]

(2) inhibits the formation of coke deposition (TGA).

Due to the similar electronegativity and electron affinity of nitrogen to carbon, nitrogen-doped carbon materials have been widely adopted. For the first time, Bao *et al.* reported that SiC supported N-doped carbon (SiC@C–N) delivers a stable performance during a 150 hours test with acetylene conversion reaching 80% and vinyl chloride selectivity over 98% at 200 °C and a GHSV of 30 h^{-1}.[67] By comparing the activity of SiC@N–C, polypyrrole (PPy) containing only pyrrolic N species, and C_3N_4 with mainly pyridinic N and quaternary N, combined with DFT calculations, it is revealed that the pyrrolic N species are the active sites, and the activity increases monotonically with the accessible-pyrrolic N sites (Fig. 14). High activity and stability can also be achieved with polydopamine (PDA) coated on SiC (PDA-SiC), which might also be attributed to the high proportion of pyrrolic nitrogen species in PDA.[161]

The coexistence of different N species (*e.g.* pyrrolic N, pyridinic N, quaternary N) makes it difficult to assess the respective catalytic roles; therefore, there is no consensus regarding the active site for the heteroatom-doped carbon material. For instance, Wei *et al.* reported a positive correlation between the quaternary N content and activity by comparing the catalytic performance of nitrogen-doped carbon nanotubes (NCNT) prepared from the self-decomposition of azodiisobutyronitrile and synthesized by CVD growth.[149] DFT calculation indicates that the nitrogen doping increases the nucleophilicity of CNTs and enhances the interaction between the highest occupied molecular orbital (HOMO) of NCNTs and the lowest unoccupied molecular orbital (LUMO) of C_2H_2, which enhances the adsorption of the C_2H_2 molecule through the formation of covalent bonds between C_2H_2 and NCNTs.

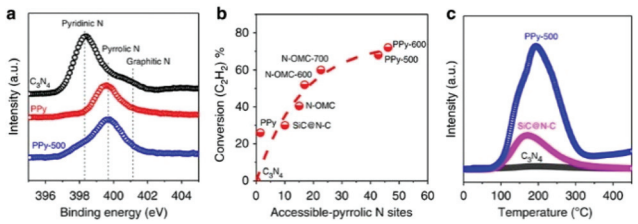

Fig. 14 (a) XPS N 1s spectra of C_3N_4, PPy and PPy-500 (PPy activated with KOH at 500 °C). (b) Acetylene conversion as a function of the accessible-pyrrolic N sites, which are estimated, for comparison, by multiplying the content of pyrrolic N species with the specific BET surface area. Reaction conditions: 200 °C, 3.1 ml g^{-1} min^{-1} and HCl/C_2H_2 = 1.15/1 (volume ratio) (c) TPD of acetylene on different catalysts. Copyright © 2014, Springer Nature.[67]

Table 4 Heteroatom-doped carbon, nitride and the corresponding precursor, N amount and possible active site

		Precursor	N amount, wt%	Active site	Ref.
1	SiC@N–C	CCl_4, NH_3, SiC	7.1	Pyrrolic N	67
	PDA/SiC	Polydopamine, SiC	4.3	Pyrrolic N	161
2	PANI-AC	Polyaniline, AC	2.39	Pyrrolic N	154
	AC-*n*-U500	Urea, AC	4.04	Pyrrolic N, Quaternary N	156
	N-CNT	CVD, C_2H_4, acetonitrile	4.4	Quaternary N	149
	PSAC-N	Melamine, spherical AC	5.04	Quaternary N	152
	N–G	NH_3, GO	5.47		153
	N-OMC	Urea, sucrose, SBA-15	3.4	Quaternary N	163
	N-OMC	phenolic resin, SBA-15, polyurethane, NH_3	4.4		159
3	N-Carbon	ZIF-8		C atoms bond to pyridinic N	162
	Z_4M_1	Melamine, ZIF-8	1.56		155
	ZIF-8/SAC	ZIF-8	1.1	Pyrrolic N	157
4	B,N–G	H_3BO_3, NH_3, GO	10.96		153
	S,N–C	Phenyldiamine $(NH_4)_2S_2O_8$	7.91	Pyrrolic N	158
	NS–C–NH_3	Sucrose, SBA-15, benzyl disulfide	18.26	C atoms bond to pyridinic N	160
5	g-C_3N_4–Cu/AC	Cyanamide, AC	7.28	Pyrrolic N	167
	g-C_3N_4/AC p-BN	Cyanamide, AC Boric acid, melamine, NH_3	8.64	Pyridinic N	151 66

So far, nitrogen-doped carbon materials with a variety of doping precursors (*e.g.* polyaniline,[154] urea,[156] melamine,[152] or NH_3[153,159]), derived from metal–organic framework (MOF) precursors such as zeolitic imidazolate framework (ZIF-8),[155,157,162] with interconnected mesoporous networks [*e.g.* ordered mesoporous carbon (OMC)][159,163] have been explored (Table 4).

Moreover, a dual doping strategy was adopted to enhance the catalytic activity. For instance, Zhu *et al.* reported that boron and nitrogen-doped oxide graphene (B,N–G) exhibited a high acetylene conversion of 94.87% and selectivity to vinyl chloride (above 98%) with a GHSV of 36 h^{-1} and at 150 °C, which might be attributed to the improved HCl adsorption.[153] The TOF of B,N–G is 3.32×10^{-2} min^{-1}, about 15% of Hg/AC and 0.6% of Au/AC (Fig. 15). The DFT calculation indicates that the adsorption energy of HCl over B,N–G is higher than that for N–G in all three types of N, with the HCl adsorption capability decreasing in the following order: pyridinic N > pyrrolic N > graphitic nitrogen.

Likewise, much attention has been paid to sulfur and nitrogen co-doped carbon materials due to the synergistic effect between S and N atoms.[158] Li *et al.* reported that C atoms bonded with pyridinic N function as the active sites based on the XPS analysis.[160] The DFT calculation demonstrates that the charge density increases along the direction from the C atom (the one between N and S) to the N atom structure in the

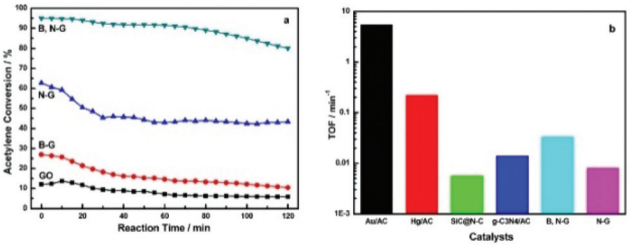

Fig. 15 (a) Catalytic reactivity evaluation of GO, B–G, N–G and B,N–G. Reaction conditions: 150 °C, atmospheric pressure, GHSV of 36 h^{-1}, HCl/C_2H_2 = 1.15/1 (volume ratio). (b)The TOFs for different catalysts: Au/AC, Hg/AC, SiC@N–C, gC_3N_4/AC, B,N–G, and N–G. Reprinted with permission from Ref. 153 Copyright 2015 American Chemical Society.[153]

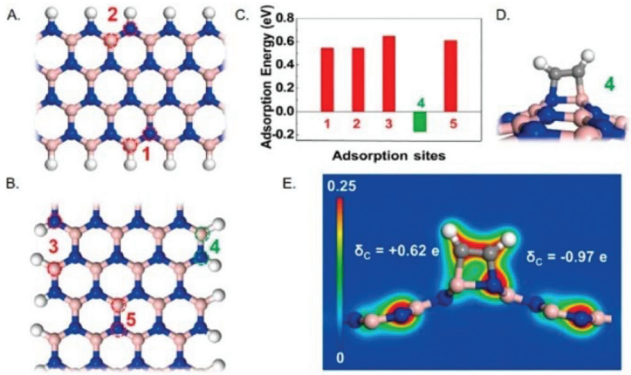

Fig. 16 DFT calculations showing different sites for acetylene adsorption. (A) Possible sites on the zigzag edge. (B) Possible sites on the armchair edge and in the plane. (C) Adsorption energies on different sites. (D) Optimized structure for acetylene adsorption on site 4 on the armchair edge. (E) Charge distribution upon adsorption of acetylene on site 4. Blue: nitrogen atoms, light pink: boron atoms, gray: carbon atoms, white: hydrogen atoms. Reprinted with permission from Ref. 66. Copyright 2017 American Chemical Society.

models of pyridinic N adjacent to the sulfide groups, indicating that C atoms adjacent to pyridinic N are liable to adsorb C_2H_2 molecules.

In addition, nitrides (*e.g.* graphitic carbon nitride and boron nitride) have gained a great deal of attention. Through DFT calculation, Dai *et al.* demonstrated that hydrogen chloride is adsorbed at the nitrogen atom and acetylene is adsorbed at the carbon atom of g-C_3N_4/AC.[151] The electron density of the nitrogen atom affects the adsorption of hydrogen chloride molecules due to the electron transfer, and the electron density on the HOMO of the pyridinic nitrogen atom is higher than those of graphitic nitrogen and primary amine groups; thus, the hydrogen chloride molecule is more readily adsorbed at the pyridinic nitrogen. Similarly, Bao and co-workers reported that porous boron nitride (p-BN) exhibits a high acetylene conversion of 99%, and a selectivity to vinyl chloride of 99% at 280 °C and a GHSV of 44 h^{-1}, which might be attributed to the abundant defects and edge sites.[66] DFT calculations indicate that the B–N sites in the armchair edge polarize and activate acetylene molecules (Fig. 16), which then react with gaseous HCl to yield VCM.

Afterwards, AC-supported transition metal nitrides (TMNs) (*e.g.* VN, Mo_2N, and W_2N,[164] Mo–Ti–N[165]) have also been explored due to the merits such as the surplus of electrons provided by N, high thermal stability, high chemical stability, high corrosion resistance and platinum-like electronic structures. Dai *et al.* reported that the conversion rate of Mo_2N/AC is higher than that of W_2N/AC and VN/AC, and proposed that the activation of reactants is related to TMNs instead of the N content.[164] Additionally, Dai *et al.* found that the doping of Ti in Mo_2N reduces the adsorption of C_2H_2 and enhances the adsorption of HCl, with the highest acetylene conversion achieved at the optimal mole ratio of Mo/Ti of 3 : 1.[165]

More recently, acetylene hydrochlorination over zeolites has also been investigated. Liu *et al.* reported that zeolite 13× exhibited high activity and selectivity in acetylene hydrochlorination above 300 °C, which might be attributed to the uniform micropores and unique supercage structure, and sodium cations and the active carbon deposit formed in the beginning of reactions facilitated acetylene hydrochlorination (Fig. 17).[166]

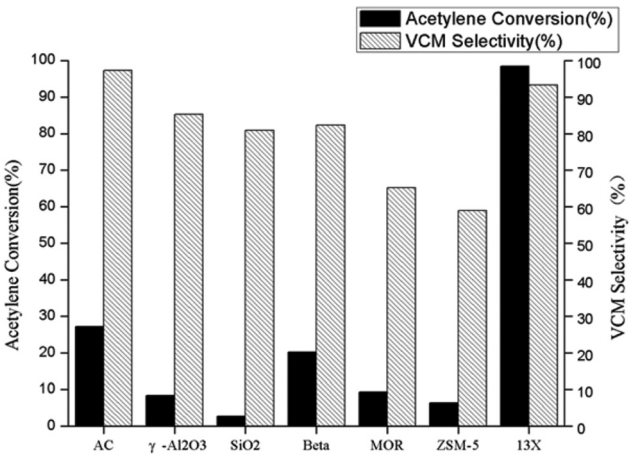

Fig. 17 Catalytic performances of different catalysts compared to 13×. Reactor set point temperature = 320 °C. Reproduced from Ref. 166 with permission from The Royal Society of Chemistry.[166]

6. Conclusion and outlook

Non-mercury catalysts for acetylene hydrochlorination are of great significance for the synthesis of VCM in terms of green chemistry. The aim of this tutorial review is to discuss the design criteria for mercury-free catalysts, with the focus on the relationship between the catalytic activity/stability and the electronic properties, adsorption and reducibility of the catalyst, and we hope this review will shed light on the rational design of heterogeneous mercury-free catalysts, and inspire more novel research to tap the potential and overcome the challenges associated with mercury-free catalysts. Eventually, the developing directions of mercury-free catalysts in acetylene hydrochlorination are predicted.

(1) There have been great achievements in Au-based catalysts, and companies such as Johnson Matthey have provided significant contribution to the promotion of Au-based catalysts. However, the relatively high price of Au-based catalysts prevents the further large-scaled commercialization and industrial application. Therefore, the exploration of cost-effective non-precious metal-based catalysts (*e.g.* Cu-based catalysts, Bi-based catalysts) and metal-free catalysts (*e.g.* nitrogen-doped carbon materials and zeolites) is of great practical significance. Moreover, it should be noted that the reaction mechanism of non-precious metal-based catalysts and metal-free catalysts might not be identical to that of noble metal based catalysts (*e.g.* Au-based catalyst), thus the deep understanding of the reaction mechanism and correlation of the catalytic activity with the active site over non-precious metal-based catalysts and metal-free catalysts will facilitate the research and development (R&D) of non-mercury catalysts.

(2) The comprehensive economic evaluation of the R&D and promotion of non-mercury catalysts. The mercury-free catalytic systems should not only be technically but also economically feasible. The operating cost of non-mercury catalysts should be within the acceptable range in the existing PVC manufacturers located in areas with vast coal reserves with oil and gas shortage, which will be beneficial for the large-scale promotion and industrial application of mercury-free catalysts in PVC production with the calcium carbide-based process.

(3) The full consideration of the technical issues of the replacement of mercury-containing catalysts with mercury-free catalysts. The optimal operating conditions (*e.g.* reaction temperature, GHSV and pressure) of the newly-developed mercury-free catalysts might be different from the existing process of mercury-containing catalysts; thus, it is of great necessity to focus on the development and optimization of the corresponding chemical processes for mercury-free catalysts. Meanwhile, the innovation in the chemical processes might, in turn, promote the R&D of the non-mercury catalysts, and facilitate the large-scaled industrial application of non-mercury catalysts.

(4) The chemical (*e.g.* the organic functional groups and impurities) and physical properties (*e.g.* the porosity and mechanical strength) of the commonly adopted support, activated carbon, have a great influence on the catalytic activity, especially the chemical/thermal stability of mercury-free catalytic systems. Therefore, it is of great significance to deeply investigate the preparation and modification strategies of activated carbon, which is beneficial for not only the stabilization and dispersion of the active component in catalytic systems but also the prevention of catalyst deactivation.

(5) The *in situ*/operando characterization of the catalyst under real reaction conditions can provide vital information on the catalytically active site. However, for the acetylene hydrochlorination, reactants are highly corrosive and/or tend to explode under pressure. Therefore, the development of the advanced *in situ*/operando characterization technique of catalytic systems under complicated real reaction conditions (*e.g.* under the circumstance that reactants are highly corrosive and/or tend to explode under pressure) is of great necessity.

Conflicts of interest

There are no conflicts to declare.

Acknowledgements

This work was supported by the State Key Research and Development Project of China (2016YFB0301603).

Notes and references

1 E.-L. Dreher, T. R. Torkelson and K. K. Beutel, in *Ullmann's Encyclopedia of Industrial Chemistry*, Wiley-VCH Verlag GmbH & Co. KGaA, 2000.
2 R. L. Myers, *The 100 Most Important Chemical Compounds: A Reference Guide*, Greenwood Press, 2007.
3 H. Schobert, *Chem. Rev.*, 2014, **114**, 1743–1760.
4 G. S. James, in *Chemical Process and Design Handbook*, McGraw Hill Professional, Access Engineering, 2002.
5 Polyvinyl Chloride (PVC) - Market Study|Ceresana, http://www.ceresana.com/en/market-studies/plastics/polyvinyl-chloride/.
6 R. Lin, A. P. Amrute and J. Perez-Ramirez, *Chem. Rev.*, 2017, **117**, 4182–4247.
7 J. G. Speight, in *Handbook of Industrial Hydrocarbon Processes*, Gulf Professional Publishing, Boston, 2011, pp. 429–466.
8 B. Yan, W. Lu and Y. Cheng, *Green Process. Synth.*, 2012, **1**, 33.
9 Foreign Economic Cooperation Office, in *R&D Progress of and Feasibility Study Report on Mercury-free Catalyst in China*, Foreign Economic Cooperation Office, Ministry of Environmental Protection, People's Republic of China, 2011.
10 United Nations Environment Programme, Minamata Convention on Mercury, http://www.mercuryconvention.org/.
11 Y. Lin, S. X. Wang, Q. R. Wu and T. Larssen, *Environ. Sci. Technol.*, 2016, **50**, 2337–2344.
12 P. Anastas and N. Eghbali, *Chem. Soc. Rev.*, 2010, **39**, 301–312.
13 R. A. Sheldon, *Chem. Commun.*, 2008, 3352–3365.
14 P. T. Anastas and M. M. Kirchhoff, *Acc. Chem. Res.*, 2002, **35**, 686–694.
15 J. H. Clark, *Green Chem.*, 1999, **1**, 1–8.
16 P. Johnston, N. Carthey and G. J. Hutchings, *J. Am. Chem. Soc.*, 2015, **137**, 14548–14557.
17 G. Malta, S. J. Freakley, S. A. Kondrat and G. J. Hutchings, *Chem. Commun.*, 2017, **53**, 11733–11746.
18 M. Conte and G. J. Hutchings, in *Modern Gold Catalyzed Synthesis*, Wiley-VCH Verlag GmbH & Co. KGaA, 2012, pp. 1–26.
19 C. J. Davies, P. J. Miedziak, G. L. Brett and G. J. Hutchings, *Chin. J. Catal.*, 2016, **37**, 1600–1607.
20 G. J. Hutchings, *Top. Catal.*, 2014, **57**, 1265–1271.

21 G. J. Hutchings, *Gold Bull.*, 2009, **42**, 260–266.
22 G. J. Hutchings, *Chem. Commun.*, 2008, 1148–1164.
23 G. J. Hutchings, *Catal. Today*, 2002, **72**, 11–17.
24 G. J. Hutchings, *Gold Bull.*, 1996, **29**, 123–130.
25 G. J. Hutchings, *Top. Catal.*, 2008, **48**, 55–59.
26 M. Zhu, Q. Wang, K. Chen, Y. Wang, C. Huang, H. Dai, F. Yu, L. Kang and B. Dai, *ACS Catal.*, 2015, **5**, 5306–5316.
27 J. Zhang, N. Liu, W. Li and B. Dai, *Front. Chem. Sci. Eng.*, 2011, **5**, 514–520.
28 I. T. Trotus, T. Zimmermann and F. Schuth, *Chem. Rev.*, 2014, **114**, 1761–1782.
29 R. Ciriminna, E. Falletta, C. Della Pina, J. H. Teles and M. Pagliaro, *Angew. Chem., Int. Ed.*, 2016, **55**, 14209–14216.
30 O. Vaughan, *Nat. Nanotechnol.*, 2010, **5**, 5–7.
31 C. Corti and R. Holliday, *Gold: science and applications*, CRC Press, 2009.
32 G. Hutchings, *Nat. Chem.*, 2009, **1**, 584–584.
33 A. S. K. Hashmi and G. J. Hutchings, *Angew. Chem., Int. Ed.*, 2006, **45**, 7896–7936.
34 S. J. Freakley, Q. He, C. J. Kiely and G. J. Hutchings, *Catal. Lett.*, 2015, **145**, 71–79.
35 G. J. Hutchings, *Catal. Today*, 2005, **100**, 55–61.
36 G. J. Hutchings and M. Haruta, *Appl. Catal., A*, 2005, **291**, 2–5.
37 G. C. Bond and D. T. Thompson, *Catal. Rev.*, 1999, **41**, 319–388.
38 A. Arcadi, *Chem. Rev.*, 2008, **108**, 3266–3325.
39 T. Takei, T. Akita, I. Nakamura, T. Fujitani, M. Okumura, K. Okazaki, J. Huang, T. Ishida and M. Haruta, in *Adv. Catal.*, Academic Press, 2012, vol. 55, pp. 1–126.
40 J. Huang, T. Takei, T. Akita, H. Ohashi and M. Haruta, *Appl. Catal., B*, 2010, **95**, 430–438.
41 J. H. Huang, T. Akita, J. Faye, T. Fujitani, T. Takei and M. Haruta, *Angew. Chem., Int. Ed.*, 2009, **48**, 7862–7866.
42 D. Thompson, *Gold Bull.*, 1998, **31**, 111–118.
43 D. M. Smith, P. M. Walsh and T. L. Slager, *J. Catal.*, 1968, **11**, 113–130.
44 K. Shinoda, *Chem. Lett.*, 1975, **4**, 219–220.
45 G. Hutchings, *J. Catal.*, 1985, **96**, 292–295.
46 B. Nkosi, N. J. Coville and G. J. Hutchings, *J. Chem. Soc., Chem. Commun.*, 1988, 71–72.
47 B. Nkosi, N. J. Coville and G. J. Hutchings, *Appl. Catal.*, 1988, **43**, 33–39.
48 B. Nkosi, M. D. Adams, N. J. Coville and G. J. Hutchings, *J. Catal.*, 1991, **128**, 378–386.
49 B. Nkosi, N. J. Coville, G. J. Hutchings, M. D. Adams, J. Friedl and F. E. Wagner, *J. Catal.*, 1991, **128**, 366–377.
50 M. Conte, A. F. Carley and G. J. Hutchings, *Catal. Lett.*, 2008, **124**, 165–167.
51 M. Conte, C. J. Davies, D. J. Morgan, T. E. Davies, D. J. Elias, A. F. Carley, P. Johnston and G. J. Hutchings, *J. Catal.*, 2013, **297**, 128–136.
52 M. Conte, A. F. Carley, C. Heirene, D. J. Willock, P. Johnston, A. A. Herzing, C. J. Kiely and G. J. Hutchings, *J. Catal.*, 2007, **250**, 231–239.
53 X. Qi, W. Li, J. Gu, C. Guo and J. Zhang, *RSC Adv.*, 2016, **6**, 105110–105118.
54 K. Zhou, W. Wang, Z. Zhao, G. Luo, J. T. Miller, M. S. Wong and F. Wei, *ACS Catal.*, 2014, **4**, 3112–3116.
55 X. Tian, G. Hong, B. Jiang, F. Lu, Z. Liao, J. Wang and Y. Yang, *RSC Adv.*, 2015, **5**, 46366–46371.
56 G. Hong, X. Tian, B. Jiang, Z. Liao, J. Wang, Y. Yang and J. Zheng, *Rsc Adv.*, 2016, **6**, 3806–3814.
57 J. Oliver-Meseguer, A. Domenech-Carbo, M. Boronat, A. Leyva-Perez and A. Corma, *Angew. Chem., Int. Ed.*, 2017, **56**, 6435–6439.
58 B. Dai, X. Li, J. Zhang, F. Yu and M. Zhu, *Chem. Eng. Sci.*, 2015, **135**, 472–478.
59 M. Conte, C. J. Davies, D. J. Morgan, T. E. Davies, A. F. Carley, P. Johnston and G. J. Hutchings, *Catal. Sci. Technol.*, 2013, **3**, 128–134.
60 M. Conte, C. J. Davies, D. J. Morgan, A. F. Carley, P. Johnston and G. J. Hutchings, *Catal. Lett.*, 2014, **144**, 1–8.
61 X. Liu, M. Conte, D. Elias, L. Lu, D. J. Morgan, S. J. Freakley, P. Johnston, C. J. Kiely and G. J. Hutchings, *Catal. Sci. Technol.*, 2016, **6**, 5144–5153.
62 J. Zhao, Y. Yu, X. Xu, S. Di, B. Wang, H. Xu, J. Ni, L. Guo, Z. Pan and X. Li, *Appl. Catal., B*, 2017, **206**, 175–183.
63 G. Malta, S. A. Kondrat, S. J. Freakley, C. J. Davies, L. Lu, S. Dawson, A. Thetford, E. K. Gibson, D. J. Morgan, W. Jones, P. P. Wells, P. Johnston, C. R. A. Catlow, C. J. Kiely and G. J. Hutchings, *Science*, 2017, **355**, 1399–1402.
64 S. Wang, B. Shen and Q. Song, *Catal. Lett.*, 2010, **134**, 102–109.
65 J. Ma, S. Wang and B. Shen, *React. Kinet., Mech. Catal.*, 2013, **110**, 177–186.
66 P. Li, H. Li, X. Pan, K. Tie, T. Cui, M. Ding and X. Bao, *ACS Catal.*, 2017, **7**, 8572–8577.
67 X. Li, X. Pan, L. Yu, P. Ren, X. Wu, L. Sun, F. Jiao and X. Bao, *Nat. Commun.*, 2014, **5**, 3688.
68 M. Zhu, L. Kang, Y. Su, S. Zhang and B. Dai, *Can. J. Chem.*, 2013, **91**, 120–125.
69 S. Shang, W. Zhao, Y. Wang, X. Li, J. Zhang, Y. Han and W. Li, *ACS Catal.*, 2017, **7**, 3510–3520.
70 T. V. Krasnyakova, I. V. Zhikharev, R. S. Mitchenko, V. I. Burkhovetski, A. M. Korduban, T. V. Kryshchuk and S. A. Mitchenko, *J. Catal.*, 2012, **288**, 33–43.
71 Y. Han, M. Sun, W. Li and J. Zhang, *Phys. Chem. Chem. Phys.*, 2015, **17**, 7720–7730.
72 J. Zhang, Z. He, W. Li and Y. Han, *RSC Adv.*, 2012, **2**, 4814–4821.
73 A. S. K. Hashmi, *Gold Bull.*, 2003, **36**, 3–9.
74 N. A. Carthey, P. Johnston and M. L. Smidt, *WIPO Pat.*, WO2010/055341(A2), 2010.
75 X. Duan, Y. Yin, X. Tian, J. Ke, Z. Wen, J. Zheng, M. Hu, L. Ye and Y. Yuan, *Chin. J. Catal.*, 2016, **37**, 1794–1803.
76 X. Duan, X. Tian, J. Ke, Y. Yin, J. Zheng, J. Chen, Z. Cao, Z. Xie and Y. Yuan, *Chem. Sci.*, 2016, **7**, 3181–3187.
77 C. University, *Gold Catalysts for Vinyl Chloride Manufacture, Research Excellence Framework 2014*, Cardiff University, 2014.

78 P. T. Bishop, N. A. Carthey and P. Johnston, *WIPO Pat.*, WO2013/008004(A3), 2013.
79 http://www.jmprotech.com/licensed-processes-vinyl-chloride-monomer, VINYL CHLORIDE MONOMER (VCM).
80 K. Zhou, J. Jia, C. Li, H. Xu, J. Zhou, G. Luo and F. Wei, *Green Chem.*, 2015, **17**, 356–364.
81 X. Yin, C. Huang, L. Kang, M. Zhu and B. Dai, *Catal. Sci. Technol.*, 2016, **6**, 4254–4259.
82 H. Xu, K. Zhou, J. Si, C. Li and G. Luo, *Catal. Sci. Technol.*, 2016, **6**, 1357–1366.
83 C. Huang, M. Zhu, L. Kang and B. Dai, *Catal. Commun.*, 2014, **54**, 61–65.
84 Y. Dong, W. Li, Z. Yan and J. Zhang, *Catal. Sci. Technol.*, 2016, **6**, 7946–7955.
85 J. Zhao, B. Wang, X. Xu, Y. Yu, S. Di, H. Xu, Y. Zhai, H. He, L. Guo, Z. Pan and X. Li, *J. Catal.*, 2017, **350**, 149–158.
86 W. Lin, R.-W. Zhang, S.-S. Jang, C.-P. Wong and J.-I. Hong, *Angew. Chem., Int. Ed.*, 2010, **49**, 7929–7932.
87 X. Li, M. Zhu and B. Dai, *Appl. Catal., B*, 2013, **142**, 234–240.
88 Y. Pu, J. Zhang, L. Yu, Y. Jin and W. Li, *Appl. Catal., A*, 2014, **488**, 28–36.
89 N. Xu, M. Zhu, J. Zhang, H. Zhang and B. Dai, *RSC Adv.*, 2015, **5**, 86172–86178.
90 L. Hou, J. Zhang, Y. Pu and W. Li, *RSC Adv.*, 2016, **6**, 18026–18032.
91 H. Zhang, W. Li, Y. Jin, W. Sheng, M. Hui, X. Wang and J. Zhang, *Appl. Catal., B*, 2016, **189**, 56–64.
92 G. Li, W. Li, H. Zhang, Y. Pu, M. Sun and J. Zhang, *RSC Adv.*, 2015, **5**, 9002–9008.
93 S. A. Mitchenko, T. V. Krasnyakova, R. S. Mitchenko and A. N. Korduban, *J. Mol. Catal. A: Chem.*, 2007, **275**, 101–108.
94 S. A. Mitchenko, E. V. Khomutov, A. A. Shubin and Y. M. Shul'ga, *J. Mol. Catal. A: Chem.*, 2004, **212**, 345–352.
95 L. A. Sil'chenko, S. A. Panova, G. K. Shestakov and O. N. Temkin, *Kinet. Catal.*, 1998, **39**, 24–28.
96 S. A. Mitchenko, *Kinet. Catal.*, 1998, **39**, 859–862.
97 S. A. Panova, G. K. Shestakov and O. N. Temkin, *J. Chem. Soc., Chem. Commun.*, 1994, **7**, 977–977.
98 L. Wang, F. Wang, J. Wang, X. Tang, Y. Zhao, D. Yang, F. Jia and T. Hao, *React. Kinet., Mech. Catal.*, 2013, **110**, 187–194.
99 L. Wang, F. Wang and J. D. Wang, *Catal. Commun.*, 2015, **65**, 41–45.
100 L. Wang, F. Wang and J. D. Wang, *New J. Chem.*, 2016, **40**, 3019–3023.
101 L. Wang, F. Wang and J. D. Wang, *Catal. Commun.*, 2016, **74**, 55–59.
102 J. Hu, Q. Yang, L. Yang, Z. Zhang, B. Su, Z. Bao, Q. Ren, H. Xing and S. Dai, *ACS Catal.*, 2015, **5**, 6724–6731.
103 K. Zhou, J. Si, J. Jia, J. Huang, J. Zhou, G. Luo and F. Wei, *RSC Adv.*, 2014, **4**, 7766–7769.
104 H. Li, F. M. Wang, W. Cai, J. Zhang and X. Zhang, *Catal. Sci. Technol.*, 2015, **5**, 5174–5184.
105 G. Qin, Y. Song, R. Jin, J. Shi, Z. Yu and S. Cao, *Green Chem.*, 2011, **13**, 1495–1498.
106 W. L. Zhao, M. Y. Zhu and B. Dai, *Catal. Commun.*, 2017, **98**, 22–25.
107 D. Hu, F. Wang and J. Wang, *RSC Adv.*, 2017, **7**, 7567–7575.
108 M. Conte, A. F. Carley, G. Attard, A. A. Herzing, C. J. Kiely and G. J. Hutchings, *J. Catal.*, 2008, **257**, 190–198.
109 Y. Jin, G. Li, J. Zhang, Y. Pu and W. Li, *RSC Adv.*, 2015, **5**, 37774–37779.
110 H. Zhang, B. Dai, X. Wang, W. Li, Y. Han, J. Gu and J. Zhang, *Green Chem.*, 2013, **15**, 829–836.
111 Y. Du, R. Hu, Y. Jia, Q. Zhou, W. Meng and J. Yang, *J. Ind. Eng. Chem.*, 2016, **37**, 32–41.
112 G. Li, W. Li and J. Zhang, *Catal. Sci. Technol.*, 2016, **6**, 3230–3237.
113 J. Xu, J. Zhao, T. Zhang, X. Di, S. Gu, J. Ni and X. Li, *RSC Adv.*, 2015, **5**, 38159–38163.
114 H. Zhang, W. Li, X. Li, W. Zhao, J. Gu, X. Qi, Y. Dong, B. Dai and J. Zhang, *Catal. Sci. Technol.*, 2015, **5**, 1870–1877.
115 J. Zhao, J. Xu, J. Xu, J. Ni, T. Zhang, X. Xu and X. Li, *ChemPlusChem*, 2015, **80**, 196–201.
116 Y. Pu, J. Zhang, X. Wang, H. Zhang, L. Yu, Y. Dong and W. Li, *Catal. Sci. Technol.*, 2014, **4**, 4426–4432.
117 J. Zhao, T. Zhang, X. Di, J. Xu, S. Gu, Q. Zhang, J. Ni and X. Li, *Catal. Sci. Technol.*, 2015, **5**, 4973–4984.
118 J. Zhao, X. Cheng, L. Wang, R. Ren, J. Zeng, H. Yang and B. Shen, *Catal. Lett.*, 2014, **144**, 2191–2197.
119 J. Zhao, S. Gu, X. Xu, T. Zhang, X. Di, Z. Pan and X. Li, *RSC Adv.*, 2015, **5**, 101427–101436.
120 Y. Dong, H. Zhang, W. Li, M. Sun, C. Guo and J. Zhang, *J. Ind. Eng. Chem.*, 2016, **35**, 177–184.
121 H. Zhang, B. Dai, W. Li, X. Wang, J. Zhang, M. Zhu and J. Gu, *J. Catal.*, 2014, **316**, 141–148.
122 C. Huang, M. Zhu, L. Kang, X. Li and B. Dai, *Chem. Eng. J.*, 2014, **242**, 69–75.
123 G. Li, W. Li and J. Zhang, *Catal. Sci. Technol.*, 2016, **6**, 1821–1828.
124 H. Nishikawa, D. Kawamoto, Y. Yamamoto, T. Ishida, H. Ohashi, T. Akita, T. Honma, H. Oji, Y. Kobayashi, A. Hamasaki, T. Yokoyama and M. Tokunaga, *J. Catal.*, 2013, **307**, 254–264.
125 J. Ke, Y. Zhao, Y. Yin, K. Chen, X. Duan, L. Ye and Y. Yuan, *J. Rare Earths*, 2017, **35**, 1083–1091.
126 J. Zhao, J. Zeng, X. Cheng, L. Wang, H. Yang and B. Shen, *RSC Adv.*, 2015, **5**, 16727–16734.
127 H. Zhang, B. Dai, X. Wang, L. Xu and M. Zhu, *J. Ind. Eng. Chem.*, 2012, **18**, 49–54.
128 L. Wang, B. Shen, J. Zhao and X. Bi, *Can. J. Chem. Eng.*, 2017, **95**, 1069–1075.
129 J. Zhang, W. Sheng, C. Guo and W. Li, *RSC Adv.*, 2013, **3**, 21062–21068.
130 L. Wang, F. Wang and J. Wang, *Catal. Commun.*, 2016, **83**, 9–13.
131 K. Zhou, J. Jia, X. Li, X. Pang, C. Li, J. Zhou, G. Luo and F. Wei, *Fuel Process. Technol.*, 2013, **108**, 12–18.

132 B. Wang, L. Yu, J. Zhang, Y. Pu, H. Zhang and W. Li, *RSC Adv.*, 2014, **4**, 15877–15885.
133 J. Zhao, J. Xu, J. Xu, T. Zhang, X. Di, J. Ni and X. Li, *Chem. Eng. J.*, 2015, **262**, 1152–1160.
134 B. Man, H. Zhang, J. Zhang, X. Li, N. Xu, H. Dai, M. Zhu and B. Dai, *RSC Adv.*, 2017, **7**, 23742–23750.
135 J. Zhao, T. Zhang, X. Di, J. Xu, J. Xu, F. Feng, J. Ni and X. Li, *RSC Adv.*, 2015, **5**, 6925–6931.
136 Y. Jia, R. Hu, Q. Zhou, H. Wang, X. Gao and J. Zhang, *J. Catal.*, 2017, **348**, 223–232.
137 J. Xu, J. Zhao, J. Xu, T. Zhang, X. Li, X. Di, J. Ni, J. Wang and J. Cen, *Ind. Eng. Chem. Res.*, 2014, **53**, 14272–14281.
138 D. A. Bulushev, I. Yuranov, E. I. Suvorova, P. A. Buffat and L. Kiwi-Minsker, *J. Catal.*, 2004, **224**, 8–17.
139 N. V. Plechkova and K. R. Seddon, *Chem. Soc. Rev.*, 2008, **37**, 123–150.
140 J. P. Hallett and T. Welton, *Chem. Rev.*, 2011, **111**, 3508–3576.
141 P. Wasserscheid and W. Keim, *Angew. Chem., Int. Ed.*, 2000, **39**, 3772–3789.
142 J. Zhao, S. Gu, X. Xu, T. Zhang, Y. Yu, X. Di, J. Ni, Z. Pan and X. Li, *Catal. Sci. Technol.*, 2016, **6**, 3263–3270.
143 Y. Li, Y. Dong, W. Li, Y. Han and J. Zhang, *Mol. Catal.*, 2017, **443**, 220–227.
144 W. Wittanadecha, N. Laosiripojana, A. Ketcong, N. Ningnuek, P. Praserthdam, J. R. Monnier and S. Assabumrungrat, *Appl. Catal., A*, 2014, **475**, 292–296.
145 W. Wittanadecha, N. Laosiripojana, A. Ketcong, N. Ningnuek, P. Praserthdam, J. R. Monnier and S. Assabumrungrat, *React. Kinet., Mech. Catal.*, 2014, **112**, 189–198.
146 K. Chen, L. Kang, M. Zhu and B. Dai, *Catal. Sci. Technol.*, 2015, **5**, 1035–1040.
147 X. Yang, C. Jiang, Z. Yang and J. Zhang, *J. Mater. Sci. Technol.*, 2014, **30**, 434–440.
148 X. Tian, G. Hong, Y. Liu, B. Jiang and Y. Yang, *RSC Adv.*, 2014, **4**, 36316–36324.
149 K. Zhou, B. Li, Q. Zhang, J. Huang, G. Tian, J. Jia, M. Zhao, G. Luo, D. Su and F. Wei, *ChemSusChem*, 2014, **7**, 723–728.
150 R. Lin, S. K. Kaiser, R. Hauert and J. Pérez-Ramírez, *ACS Catal.*, 2018, **8**, 1114–1121.
151 X. Li, Y. Wang, L. Kang, M. Zhu and B. Dai, *J. Catal.*, 2014, **311**, 288–294.
152 X. Wang, B. Dai, Y. Wang and F. Yu, *ChemCatChem*, 2014, **6**, 2339–2344.
153 B. Dai, K. Chen, Y. Wang, L. Kang and M. Zhu, *ACS Catal.*, 2015, **5**, 2541–2547.
154 C. Zhang, L. Kang, M. Zhu and B. Dai, *RSC Adv.*, 2015, **5**, 7461–7468.
155 X. Li, J. Zhang and W. Li, *J. Ind. Eng. Chem.*, 2016, **44**, 146–154.
156 T. Zhang, J. Zhao, J. Xu, J. Xu, X. Di and X. Li, *Chin. J. Chem. Eng.*, 2016, **24**, 484–490.
157 X. Li, J. Zhang, Y. Han, M. Zhu, S. Shang and W. Li, *J. Mater. Sci.*, 2018, **53**, 4913–4926.
158 J. Wang, F. Zhao, C. Zhang, L. Kang and M. Zhu, *Appl. Catal., A*, 2018, **549**, 68–75.
159 X. Li, X. Pan and X. Bao, *J. Energy Chem.*, 2014, **23**, 131–135.
160 X. Dong, S. Chao, F. Wan, Q. Guan, G. Wang and W. Li, *J. Catal.*, 2018, **359**, 161–170.
161 X. Li, P. Li, X. Pan, H. Ma and X. Bao, *Appl. Catal., B*, 2017, **210**, 116–120.
162 S. Chao, F. Zou, F. Wan, X. Dong, Y. Wang, Y. Wang, Q. Guan, G. Wang and W. Li, *Sci. Rep.*, 2017, **7**, 39789.
163 Y. Yang, G. Lan, X. Wang and Y. Li, *Chin. J. Catal.*, 2016, **37**, 1242–1248.
164 H. Dai, M. Zhu, H. Zhang, F. Yu, C. Wang and B. Dai, *J. Ind. Eng. Chem.*, 2017, **50**, 72–78.
165 H. Dai, M. Zhu, H. Zhang, F. Yu, C. Wang and B. Dai, *Catalysts*, 2017, **7**, 200.
166 Z. Song, G. Liu, D. He, X. Pang, Y. Tong, Y. Wu, D. Yuan, Z. Liu and Y. Xu, *Green Chem.*, 2016, **18**, 5994–5998.
167 W. Zhao, M. Zhu and B. Dai, *Catalysts*, 2016, **6**, 193.